Chapter 18
A Numerical Study on Hydrodynamic and Liquefaction Analysis of Coastline Protected with Geotubes

A. Henitha Banumathi and S. P. Jeyapriya

Introduction

Coastline erosion is a significant problem along the shoreline due to the breaking of ocean waves, change in water levels, climate change, etc., and it is the major reason for the failure of onshore structures [1]. Conventional structures like breakwaters, seawalls, revetments, and groins are generally used to reduce shoreline erosion. These structures require a large amount of natural rocks or concrete blocks which are more expensive, and it is difficult to transport [2]. Due to the shortage of natural materials, it is suggested that it can be replaced by materials like slags, geosynthetics, gabions, etc.

Geotubes

Geosystems are the new construction systems made of geotextiles in the form of geomatresses, geotubes, geocontainers, and geocurtains for shoreline protection [2–4]. Geotextiles are typically made of synthetic fabrics made from polymeric materials like poly-ester (PET), poly-propylene (PP), poly-ethylene (PE), and poly-amide (PA). It can perform three major functions such as, (a) filtration (permeable, but soil tight), (b) reinforcement for soil against sliding, and (c) prevention of erosion of subsoil.

Geotextile tubes (geotubes) are long cylindrical tubes that are placed in the required position and filled by locally available dredged materials in the form of slurry using hydraulic pumps. While filling the tubes, the excess water will drain out from the tube, and it causes the decrease of tube height from initial, so that the geotubes

A. Henitha Banumathi (✉) · S. P. Jeyapriya
Government College of Technology, Coimbatore, Tamil Nadu, India
e-mail: henithace@gmail.com

K. Muthukkumaran et al. (eds.), *Soil Dynamics, Earthquake and Computational Geotechnical Engineering*, Lecture Notes in Civil Engineering 300,
https://doi.org/10.1007/978-981-19-6998-0_18

are needed to be filled more than once till the required height is attained [5]. If the required height is not sufficient by using the single tube, then tubes can be arranged in a stacked manner [1]. The general failure mechanisms of geotube embankment are sliding and overturning of geotubes, instability of ocean floor, scouring of the toe, and failure of geotextile material [1, 6]. Several studies have been made for the sliding and overturning failures of geotubes from physical model tests and case studies. This study mainly focuses on the failure of geotubes due to the instability of the ocean floor in terms of wave-induced liquefaction.

Liquefaction

Wave-induced liquefaction is categorized into two types: (i) due to earthquake effects and (ii) due to water pressure generated by the wave propagation. The effect of the second type of liquefaction is that, when wave propagation takes place which is a dynamic pressure acting on the soil, it results in the development of excess pore pressure and effective stresses in the soil mass. The reason is that ocean waves cause rearrangement of solid particles resulting in the reduction of volume of voids [7]. When the excess pore pressure gets exceeded the critical value, the soil liquefy leading to instability of coastal structures. Even the structure gets sunk into the liquefied soil depending upon the depth of liquefiable soils [8–10]. Hence, determination of effective stress, distribution of pore pressure, interaction between soil, and waves and the geometry of the structure are very important in the study of hydrodynamic analysis. Studies showed that, longer wave periods and waves rising to greater heights will generate pore pressure of higher magnitude on the seaward side of a breakwater and there is a decrease in pore pressure was observed in the core of the breakwater [11].

On comparing the wave-induced liquefaction with that of seismically induced liquefaction, there exists two major differences, (i) ocean wave periods are longer than earthquake shaking and (ii) ocean wave loadings are imposed at the surface of the seafloor, whereas earthquakes impose loads which are below the sea floor. Hence, wave-induced liquefaction analysis can be made by making suitable modification in the earthquake-induced liquefaction analysis.

Considering pore pressure development, the rate and amount of pore pressure build-up rely on three factors such as (i) storm characteristics, (ii) cyclic loading characteristics, and (iii) drainage and compressibility characteristics of soil profile [9, 12].

The liquefied zone is different from the shear failure zone as shear failure zone is likely to occur at both toes of breakwater, whereas in the liquefied zone, the failure will occur around the wave trough with highest upward seepage force [10, 11].

Hence the objectives of the study are to create a numerical model of a coastline having severe erosion, to analyse the factors of failures with respect to different sizes of geotube embankment and different levels of groundwater and finally to analyse

Table 18.1 Soil characteristics of the study area

Characteristics	Mandaikadu
Type of soil (texture)	Sandy
Colour	Yellowish-brown
Sand %	87.5
Gravel %	5.5
Silt and clay %	7

the wave-induced liquefaction from the change in void ratio and effective stress with respect to depth.

Location and Topography of Study Area

In this study, the coastline of Mandaikadu has been chosen for the analysis. The coastline of Mandaikadu, Kalkulam Taluk, Kanyakumari District is one of the most prone zones of beach erosion which has a fishing harbour, beach sand mining, and thick fishermen habituation along the shoreline, and it is located between 8° 10′ 30.9″ to 8° 09′ 44.1″ N Latitude and 77° 15′ 35.5″ to 77° 16′ 58.8″ E Longitude along the western coast of the Arabian Sea. Wind, wave, and coastal disturbances such as storm surges, sea-level rise, and other natural processes are the main causes of erosion in the studied region. The observed predominant wind directions of the study area were SW, SSW, and N with a 0.78% calm period. The SW monsoon is severe along the coast creating heavy erosion resulting in loss of valuable lands, roads, worship places, and houses. The soil characteristics of the study area are given in Table 18.1. Along the shore side, an elevation of (+) 6.00 m was observed at about 50 m behind the shoreline. The sea bed slope up to a water depth of (−) 10.00 m is 0.0455. The foreshore slope up to a water depth of about (−) 10.00 m is 0.0455. The bed slope up to (−) 3.00 m is 0.060 indicating that the profile has a steeper slope in the shallow depth compared to deep water. This can result in a run-up of wave height ranging from 1 to 3 m and break close to the shore. Figure 18.1 shows the cross-shore profile of the study area. The details of location and topography of the study area discussed above and Tables 18.1 and 18.3 and Figs. 18.1 and 18.2 were referred from the Environmental Impact Assessment (EIA) study report by Anti Sea Erosion Division of Public Works Department, Government of Tamil Nadu [13].

Numerical Modelling of Coastline

In this study, the modelling software PLAXIS 3D (2013) is used to evaluate the performance of coastline and geotubes for various conditions. PLAXIS is a finite element package intended for the two-dimensional and three-dimensional analysis

Fig. 18.1 Cross-shore profile

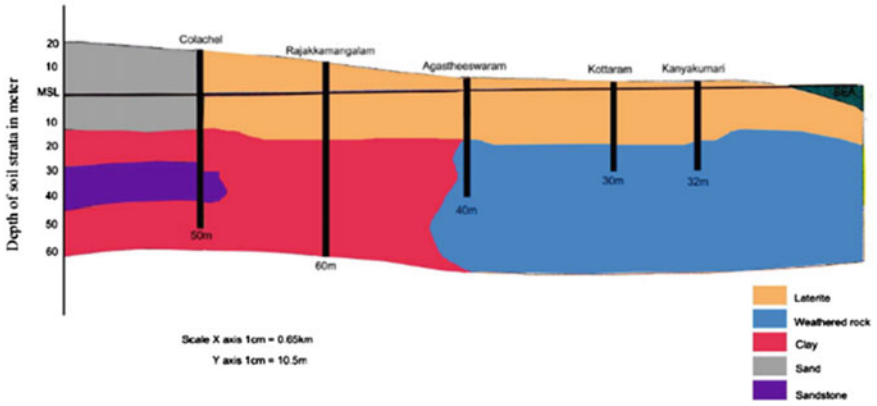

Fig. 18.2 Location of boreholes

of deformation and stability characteristics of geotechnical engineering structures. Laboratory experiments are not effective to simulate the nonlinear, time-dependent, and anisotropic behaviour of soils and/or rocks and dealing with hydrostatic and non-hydrostatic pore pressures in the soil. In the field, studies on soil and its behaviour itself is a cumbersome process in the case of tunnel projects, structures subjected to vibration and wave loading, numerical modelling simplifies the difficulties mentioned above with less cost and time. The soil properties and wave characteristics collected for the study area from various resources are given in Tables 18.2 and 18.3, respectively. Based on the data collected, a numerical model of the coastline was created having dimensions $x = 40$ m (length), $y = 10$ m (width), $z = 50$ m (depth), and the soil layers were created as per borehole data of the study area as shown in Figs. 18.2 and

18.3. Based on the cross-shore profile (Fig. 18.1) of the study area, an embankment was created on the onshore side.

The Mohr–Coulomb model was chosen to find the behaviour of soil. It is a linear elastic and perfectly plastic model and is generally used to find the first approximation of soil behaviour [14]. Numerical modelling of geotube was carried out using poly-curve option in structures mode then the shape of the curve was extruded as a tube. Totally three geotube models were created with different dimensions as shown in

Table 18.2 Properties of soil

Soil type	γ_{unsat} (kN/m^3)	γ_{sat} (kN/m^3)	k (m/day)	E (kPa)	ν	C (kPa)	Φ (deg)
Geotube fill	16.5	17.5	0.34	18,000	0.4	5	30
Topsoil	16	18	0.34	20,000	0.4	9	30
Sandy flay	15	17.5	0.86	6000	0.4	5	25
Sand	16.5	18	0.86	30,000	0.35	0	35
Kankar	19	20	0.04	360,000	0.3	35	32
Sand stone	18	19	0.34	60,000	0.32	22	30

Source Kim et al. [2]

Table 18.3 Wave characteristics of the study area

Month	Jan	Feb	Mar	Apr	May	June	July	Aug	Sept
Height of wave (m)	0.5	0.6	0.5	0.5	1.56	1.56	1.41	1.56	1.25
Time (s)	10	12	13	12	10	6	7	8	10

Source Shoreline Protection Structures, Mandaikadu, Kanyakumari District, PWD/Anti Sea Erosion Division, Govt. of Tamil Nadu

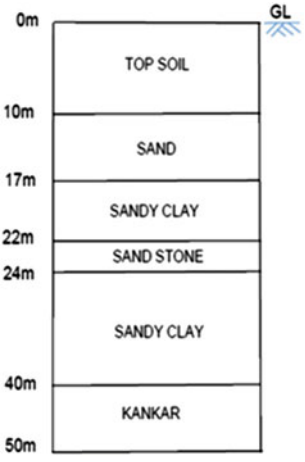

Fig. 18.3 Soil profile of study area

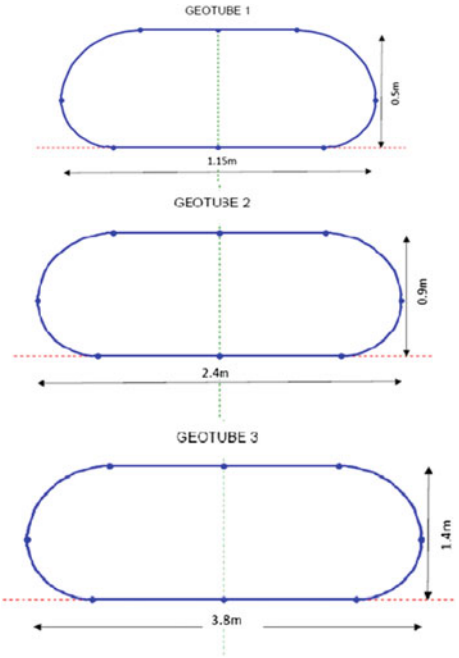

Fig. 18.4 Geotube models

Fig. 18.4, and the geotubes are assigned as a linear elastic geogrid element having axial stiffness of 600 kN/m.

Interface elements were used to simulate the exact behaviour of soil and geotube interaction. Interfaces were created for each of the geotubes and for the soil layer where the bottom of geotubes were placed. The roughness of interaction was modelled by using strength reduction factor (R_{inter}) in the material properties menu, and the values of R_{inter} was taken as 0.7 for both geotube fill and top soil [2].

For this present study, four different cases have been considered, namely

1. Coastline without geotube.
2. Coastline protected with geotube of diameter1.15 m.
3. Coastline protected with geotube of diameter 2.4 m.
4. Coastline protected with geotube of diameter 3.8 m.

In each case, analysis has been carried out for three different groundwater levels (GWL), i.e., at the ground surface, at 5 m below ground surface, at 15 m below ground surface. This is to include the variations of seepage along the shoreline. The depth of water above ground level is taken as 2 m for all the cases, and it was assigned as a harmonic flow function to simulate the ocean wave. The properties of the wave used in the analysis is given in Table 18.3.

Here, ocean wave is the dynamic load acting on the geotube embankment, and it was modelled by creating a surface water level of 2 m head and assigned as a harmonic function. For dynamic analysis, the water surface was assigned as a surface load of

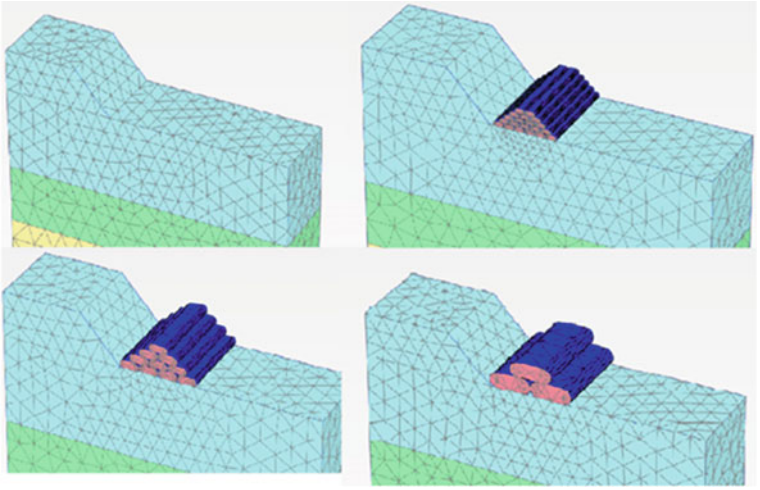

Fig. 18.5 Numerical model of the coastline

20 kN/m^2 and applied in both x and z directions as a dynamic load and activated during the dynamic analysis. After the completion of models for each case, the mesh has been generated using mesh mode. Figure 18.5 shows the numerical model of embankment along with geotubes.

Staged Construction

Staged construction is a feature to enable realistic simulation of construction, loading, and excavation processes. Starting with the initial phase, all the soil layers were activated, and K0 procedure is used for the analysis. On further phases, embankment soil, geotubes, and geotube fills were activated one by one.

Fully coupled flow deformation analysis is required when it is necessary to analyse the time-dependent development of deformations and pore pressures in saturated and partially saturated soils like drawdown of dams, dams subjected to tidal waves, dewatering of building sites, etc. [14].

Results and Discussion

From the hydrodynamic analysis, the deformed shapes of the model, total displacement of the geotube arrangement, and the global safety factors were found out for all the cases of study. Figures 18.6, 18.7 and 18.8 show the deformed shape of the model

at the end of dynamic analysis, and Figs. 18.9, 18.10 and 18.11 show the displacements of geotubes and the change in displacements. Similarly, Figs. 18.12 and 18.13 show the variation of total displacement and global safety factor respectively for different diameters of geotube.

It can be observed that, the bottom most layer of geotubes are the most unstable tubes in all the cases which attains the maximum displacement. There observed a lowering of ocean floor as noted from Figs. 18.6, 18.7 and 18.8 that proves that the reason for the maximum displacement of bottom most layer of geotube is due to the instability of ocean floor, and it lowers the total geotube arrangement.

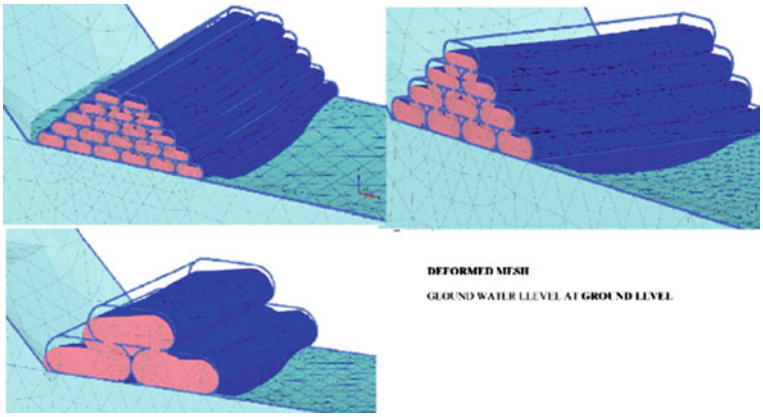

Fig. 18.6 Deformed coastline—GWL at 0 m

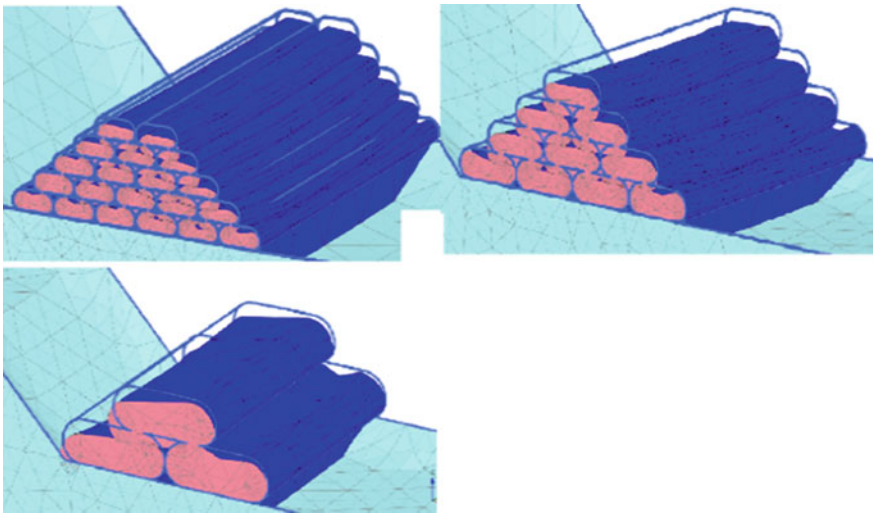

Fig. 18.7 Deformed coastline—GWL at 5 m

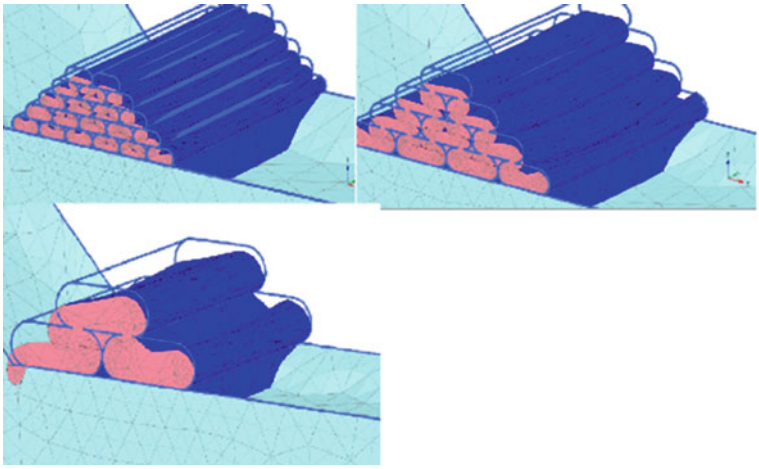

Fig. 18.8 Deformed coastline—GWL at 15 m

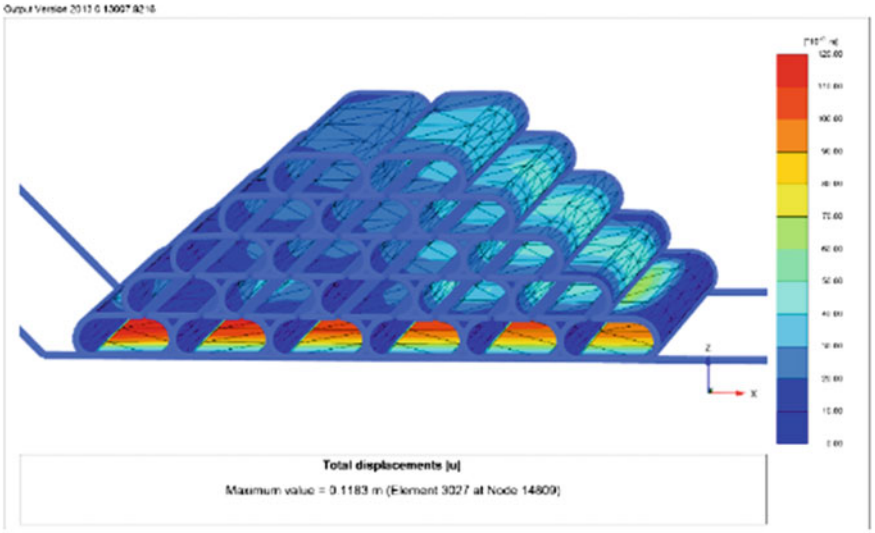

Fig. 18.9 Displacement of geotube of size 1.15 m

The smaller sizes of geotube arrangement like 1.15 and 2.4 m were found to be stable at the end of dynamic analysis but bigger size geotube arrangement, i.e., 3.8 m gets collapsed. It demonstrates that, lower geotube sizes may be densely packed towards the end of dynamic loading, resulting in a stable embankment. It is clear from Fig. 18.13 that, a higher safety factor for lower sizes of geotubes, and also it proved that the lowering of GWL increases the safety factor. Total displacement of geotubes showed that, the presence of geotubes reduces the total displacement when

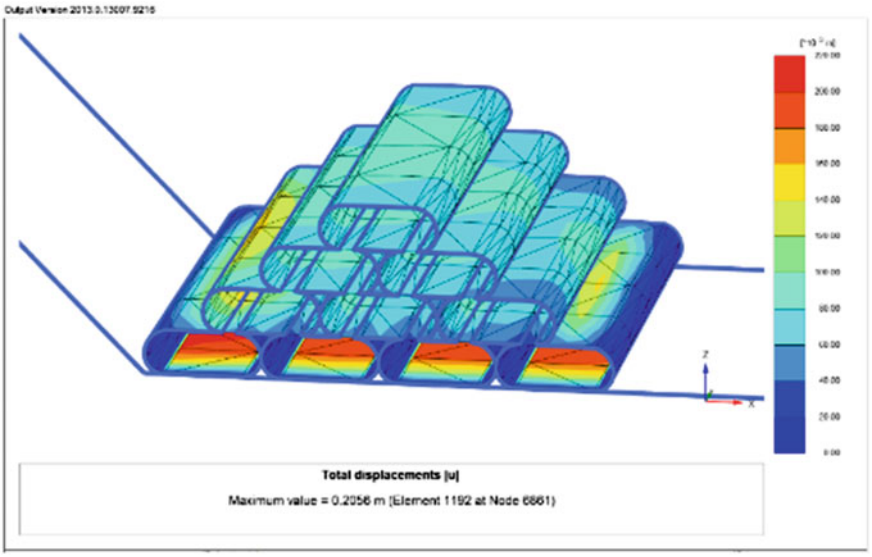

Fig. 18.10 Displacement of geotube of size 2.4 m

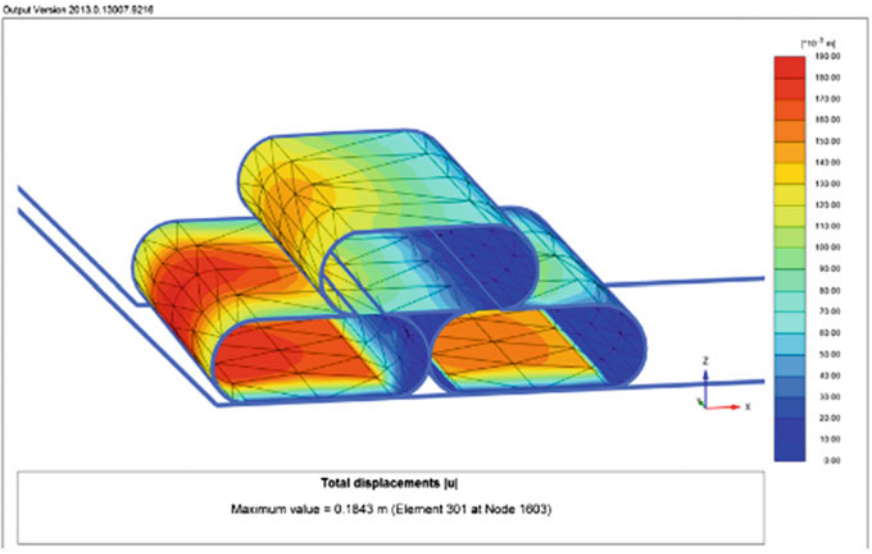

Fig. 18.11 Displacement of geotube of size 3.8 m

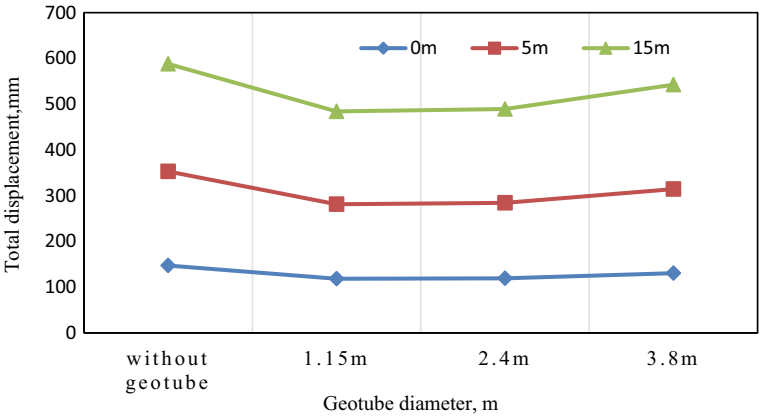

Fig. 18.12 Variation of total displacement w.r.t different diameters of geotube

compared to that of coastline without geotube as depicted in Fig. 18.12, but it shows higher displacement on lowering of GWL.

However, when GWL is much lower, the safety factor values are considerably greater, thus the geotube embankment will remain stable even if the load is increased or the strength characteristics of the bottom soil decreases.

To analyse the ocean floor instability, a comparative study was carried out for the variation of void ratio and effective stress with respect to depth for different diameters of geotubes and also with varying GWL. From the results obtained, the critical depth for liquefaction was found out. The analysis was carried out for the plane of soil at the bottom of geotube having coordinates $x = 16$–21 m, $y = 5$ m (midpoint of the width), and $z = 0$–10 m (depth of soil).

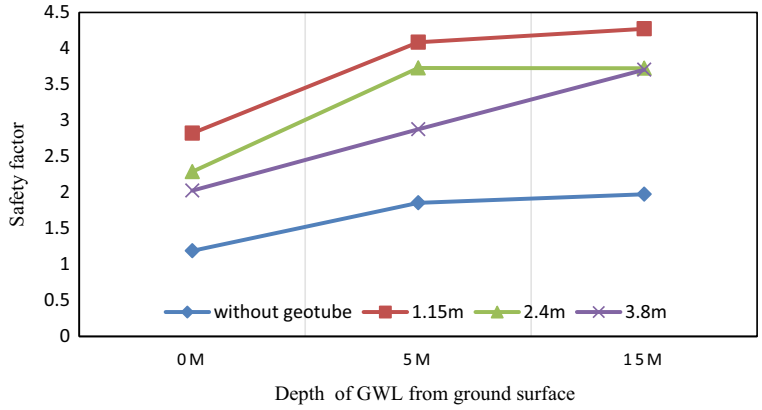

Fig. 18.13 Variation of global safety factor w.r.t depth of GWL

For each groundwater level, a relationship between the changes in void ratio vs. depth as shown in Figs. 18.14, 18.15 and 18.16 was observed and studied. In all the cases of GWL, up to a depth of 1.5 m, there is reduction in void ratio from 0.86 to 0.84 but when the GWL is nearer to the ground surface, there is more fluctuation in void ratio within the values 0.86 and 0.84.

While analysing the effective stress of the same plane of soil, the effective stress decreases on an average between 50 and 40 kN/m^2 within a depth of 0.5 m when geotube protection is not provided and thereafter it increases slowly with respect to depth. Due to the loss of effective stress, it is easy for the soil to be liquefied since the

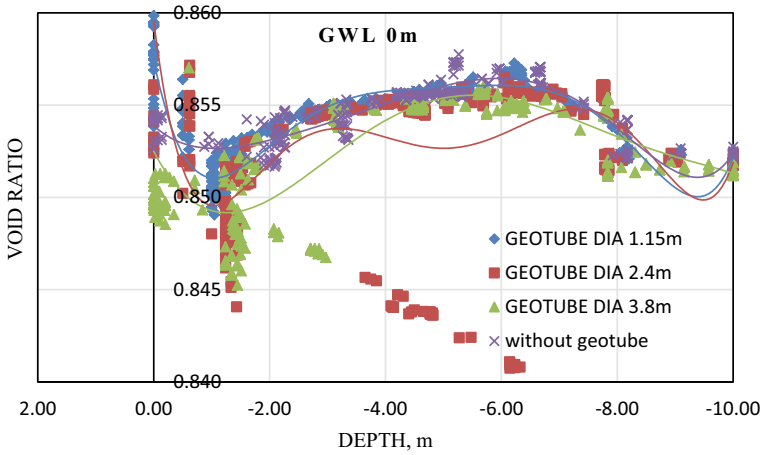

Fig. 18.14 Variation of void ratio w.r.t depth of soil when GWL 0 m

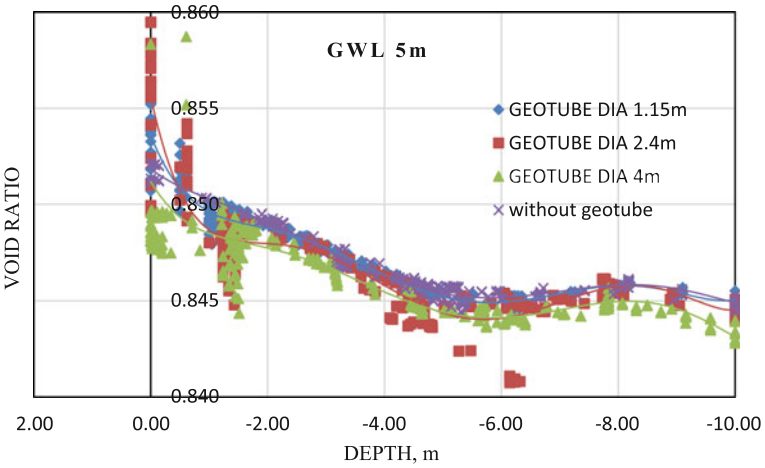

Fig. 18.15 Variation of void ratio w.r.t depth of soil when GWL 5 m

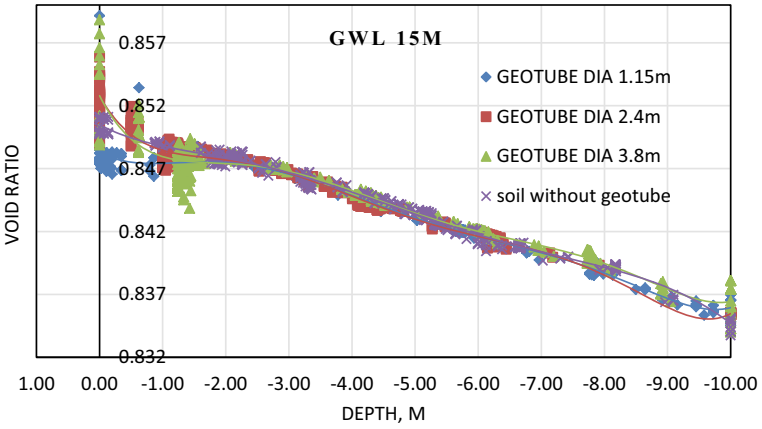

Fig. 18.16 Variation of void ratio w.r.t depth of soil when GWL 15 m

loss is within a shallow depth of 0.5 m. When there is geotube protection, the average reduction of effective stress is between 30 and 35 kN/m^2 up to a depth of 1–1.2 m. Hence, the presence of geotube increases the depth of loss of effective stress that can reduce the possibility of liquefaction of bottom soil.

Conclusions

A numerical analysis using PLAXIS 3D is performed to simulate and understand the effects of various sizes of geotube embankment with varying GWL under the action of wave loading. From the study, the following conclusions are drawn:

1. The size of the geotube has a significant effect on the stability of the geotube embankment. The smaller size of geotubes arranged in a stacked manner gives better resistance against displacement.
2. The fluctuations in groundwater level also influence the stability of geotubes. Lowering of GWL increases the total displacement of the geotube. But the safety factor values are much higher when GWL is at 15 m so the geotube embankment will be stable even on further increase of load or decrease of strength parameters of bottom soil.
3. When ocean waves propagate over a seabed, a reduction of voids ratio was observed, due to the rearrangement of the soil grains, and it decreases the effective stresses within 0.5 m and increases the possibility of liquefaction.
4. The presence of geotube embankment reduces the loss of effective stress and makes the depth of maximum loss at 1.2 m. Since the wave-induced liquefaction will occur mostly on top of the seabed, the presence of geotubes acts like a cut-off to the liquefaction.

References

1. Sherlin Prem Nishold S, Sundravadivelu Nilanjan Saha R (2018) Hydrodynamic performance of coastal geotube embankment with and without gabion boxes. Springer International Publishing AG. https://doi.org/10.1007/978-3-319-61648-3_15
2. Kim H-J, Won M-S, Jamin JC (2014) Finite-element analysis on the stability of geotextile tube—reinforced embankments under scouring. ASCE Int J Geomech. ISSN 1532-3641/06014019(13)
3. Lee SC, Hashim R, Mo KH (2018) The evaluation of geotube behaviors on muddy beach: field monitoring and numerical analysis. KSCE J Civ Eng 22(11):4185–4193
4. Pilarczyk K (1999) Geosynthetics and geosystems in hydraulic and coastal engineering, 1st edn. Rotterdam
5. Shin EC, Oh YI (2007) Coastal erosion prevention by geotextile tube technology. Geotext Geomembr 25:264–277
6. Kiran AS, Ravichandran V, Sivakholundu KM (2015) Stability analysis and design of offshore submerged breakwater constructed using sand filled geo synthetic tubes. Procedia Eng 116(2015):310–319
7. Sumer BM, Fredsøe J, Christensen S, Lind MT (1999) Sinking-floatation of pipelines and other objects in liquefied soil under waves. Coast Eng 38:53–90
8. Jeng DS, Zhang H (2005) An integrated three-dimension model of wave-induced pore pressure and effective stress in a porous seabed: II. Breaking Waves Ocean Eng 37:1950–1967
9. Bolton Seed H, Rahman MS (2008) Wave-induced pore pressure in relation to ocean floor stability of cohesion less soils. Marine Geotechnol 3(2):123–150. https://doi.org/10.1080/10641197809379798
10. Ren Y, Xu G, Xu X, Zhao T, Wang X. The initial wave-induced failure of silty seabed: liquefaction or shear failure. Science Direct. https://doi.org/10.1016/j.oceaneng.2020.106990
11. Can Ulker MB, Tatlioglu E, Aysen Lav M (2018) Dynamic response and liquefaction analysis of seabed-rubble mound breakwater system under waves. Appl Ocean Res 78(2018):75–87
12. Zhao HY, Liang ZD, Jeng D-S, Zhu JF, Guo Z, Chen WY (2018) Numerical investigation of dynamic soil response around a submerged rubble mound breakwater. Ocean Eng 156:406–423
13. Environmental Impact Assessment (EIA) report, shoreline protection structures (2011), Mandaikadu, Anti Sea Erosion Division/Public Works Department, Government of Tamil Nadu
14. PLAXIS 3D 2013 Reference manual